International Journal of Nanomedicine

Dovepress
Taylor & Francis Group

Open Access Full Text Article

ORIGINAL RESEARCH

Human Primary Monocytes as a Model for in vitro Immunotoxicity Testing: Evaluation of the Regulatory Properties of TiO_2 Nanoparticles

Tereza Svadlakova[1,2], Martina Kolackova[1], Pavel Kulich[3], Jan Kotoucek[3,4], Michaela Rosecka[1], Jan Krejsek[1], Zdeněk Fiala[2], Ctirad Andrýs[1]

[1]Department of Clinical Immunology and Allergology, University Hospital Hradec Kralove and Faculty of Medicine in Hradec Kralove, Charles University, Hradec Kralove, Czech Republic; [2]Department of Preventive Medicine, Faculty of Medicine in Hradec Kralove, Charles University, Hradec Kralove, Czech Republic; [3]Department of Pharmacology and Toxicology, Veterinary Research Institute, Brno, Czech Republic; [4]Central European Institute of Technology, Brno University of Technology, Brno, Czech Republic

Correspondence: Tereza Svadlakova, Department of Clinical Immunology and Allergology, University Hospital Hradec Kralove and Faculty of Medicine in Hradec Kralove, Charles University, Sokolska 581, Hradec Kralove, 50005, Czech Republic, Email svadlakovat@lfhk.cuni.cz

Introduction: A critical step preceding the potential biomedical application of nanoparticles is the evaluation of their immunomodulatory effects. Such nanoparticles are expected to enter the bloodstream where they can be recognized and processed by circulating monocytes. Despite the required biocompatibility, this interaction can affect intracellular homeostasis and modulate physiological functions, particularly inflammation. This study focuses on titanium dioxide (TiO_2) as an example of relatively low cytotoxic nanoparticles with potential biomedical use and aims to evaluate their possible modulatory effects on the inflammasome-based response in human primary monocytes.

Methods: Monocyte viability, phenotypic changes, and cytokine production were determined after exposure to TiO_2 (diameter, 25 nm; P25) alone. In the case of the modulatory effects, we focused on NLRP3 activation. The production of IL-1β and IL-10 was evaluated after (a) simultaneous activation of monocytes with bacterial stimuli muramyl dipeptide (MDP), or lipopolysaccharide (LPS), and TiO_2 (co-exposure model), (b) prior activation with TiO_2 alone and subsequent exposure to bacterial stimuli MDP or LPS. The differentiation of TiO_2-treated monocytes into macrophages and their polarization were also assessed.

Results: The selected TiO_2 concentration range (30–120 μg/mL) did not induce any significant cytotoxic effects. The highest dose of TiO_2 promoted monocyte survival and differentiation into macrophages, with the M2 subset being the most prevalent. Nanoparticles alone did not induce substantial production of inflammatory cytokines IL-1β, IL-6, or TNF-α. The immunomodulatory effect on NLRP3 depended on the type of costimulant used. While co-exposure of monocytes to MDP and TiO_2 boosted NLRP3 activity, co-exposure to LPS and TiO_2 inhibited NLRP3 by enhancing IL-10 release. The inhibitory effect of TiO_2 on NLRP3 based on the promotion of IL-10 was confirmed in a post-exposure model for both costimulants.

Conclusion: This study confirmed a non-negligible modulatory effect on primary monocytes in their inflammasome-based response and differentiation ability.

Keywords: TiO_2 nanoparticles, monocytes, macrophages, NLRP3, immunomodulation, polarization

Introduction

Titanium dioxide (TiO_2) nanoparticles (NPs) are among the most widely produced nanoparticles. Due to their unique physical and antimicrobial properties, they have been extensively studied for the potential use in nanomedicine with possible applications in biosensors, implantology, antitumor therapy, or as drug carriers and adjuvants.[1] Currently, TiO_2 NPs are present in multiple sectors and products, including the cosmetics, pharmaceutical, and, until recently, food articles.[2,3] The large-scale production of TiO_2 then increases occupational exposure levels, which can reach up to 5.99 mg/m^3.[4] Either way, the human exposure to TiO_2 is not negligible and requires comprehensive safety evaluation.

Received: 21 October 2024
Accepted: 7 January 2025
Published: 30 January 2025

As particles below 100 nm, TiO_2 easily pass through biological barriers.[5] The subsequent biodistribution is dependent on number of factors, eg particle size or surface charge. However, existing pharmacokinetic data remain inconsistent.[6] Although there is still a debate as to whether inhaled or ingested TiO_2 NPs are translocated through the systemic circulation to distant organs,[7–10] it is indisputable that intravenous administration offers full bioavailability.[11] Animal studies have demonstrated that TiO_2 reaches the heart, kidneys, brain, lymph nodes and thymus, with the highest retention in the liver, spleen and lungs.[11–13] Following repeated exposure, the poorly soluble nature of TiO_2 NPs may impede the elimination process, leading to its accumulation.[11,14] Nevertheless, whether during biodistribution, accumulation or elimination, TiO_2 is in constant contact the immune system.

Reducing cytotoxicity is a crucial step in attempting to utilize NPs in nanomedicine. One of the principal mechanisms of NPs cytotoxicity is the induction of inflammation, which underscores the interaction with immune cells.[15] Of these, the mononuclear phagocyte system (MPS), which consists of blood monocytes, monocyte-derived macrophages and resident macrophages, plays an effector role in the recognition and processing of NPs.[16,17] Both macrophages and monocytes are main mediators of proinflammatory and anti-inflammatory (regulatory) responses. Notably blood monocytes are greatly sensitive to a wide range of stimuli. Such capacity is enabled by the high expression of various pattern recognition receptors (PPRs), including membrane Toll-like receptors (TLRs) and intracellular Nucleotide-Binding Oligomerization Domain-like receptors (NLRs, NOD).[18] Typical stimuli are pathogen or danger-associated molecular patterns (PAMPs, DAMPs), the recognition of which leads to an activation of relevant protein complexes and transcription factors. A good example is the NLRP3 inflammasome, whose activation induces the release of potent proinflammatory cytokines interleukin (IL) −1β and IL-18. This process must be strictly regulated to prevent prolonged or persistent activation, which could result in chronic inflammation and autoimmune reactions.[19,20] Under specific condition, monocytes can "switch" their metabolic programming, leading either to the induction of innate immune memory, or tolerance.[21] In addition, during their migration to the site of inflammation, monocytes differentiate into macrophages with possible polarization into proinflammatory M1 subsets (characterized by production of IL-6, tumor necrosis factor-α (TNF-α), IL-1β, reactive oxygen species (ROS), and nitric oxide), or anti-inflammatory M2 subsets (characterized by prevailing production of IL-10 and high expression of scavenger receptors).[22–25] These changes then strongly modulate the ongoing inflammation.[26,27]

It has been shown that nanomaterials and NPs are able to modulate inflammatory homeostatic mechanisms, even without affecting the viability of cells.[21,28,29] Numerous studies have confirmed the relatively low cytotoxicity of TiO_2 in vitro and in vivo; despite the common induction of ROS.[30–33] Several studies have proposed a proinflammatory effect on macrophages.[34,35] Nevertheless, a few studies have postulated modulatory effect of TiO_2 in the presence of another stimulus, implying an interference with aforementioned homeostatic mechanisms.[36–38] The research focused on multiple stimulus is necessary, because immune cells usually react to more than one stimulus and NPs are often contaminated. Furthermore, it may reveal the potential proinflammatory effect of those NPs that do not appear to cause any acute cytotoxic response on their own.

To date, experiments have mainly been performed using cancer cell lines (THP-1, RAW264.7, etc)., which tend to be less sensitive.[39] On the contrary, human primary monocytes are often neglected, even though their role in inflammatory processes during NPs penetration into the blood is crucial. Therefore, our study established primary monocytes as a highly sensitive model for evaluating the immunomodulatory effects of TiO_2 nanoparticles. Specifically, we aimed to investigate the inflammasome-based response to TiO_2 in the presence of common bacterial fragments, muramyl dipeptide (MDP), and lipopolysaccharide (LPS), and the effect of TiO_2 on monocyte differentiation.

Materials and Methods

Nanoparticles Preparation and Characterization

TiO_2 nanoparticles (P25; anatase/rutile mixture, Product no. 718467, LOT MKCD 8503) were obtained as powder from Sigma-Aldrich (USA). Detailed physicochemical characterization, including data from X-ray diffraction, Raman spectrometry, and atomic force microscopy, was recently published by Bacova et al.[30]

Stock suspension of TiO_2 (1 mg/mL) was prepared by sonication in distilled water using ultrasonic probe (Q700 ultrasonic processor with a 1/4″ microtip probe, 15 min at 65% of amplitude; QSonica, USA). The shape and size were determined by transmission electron microscopy (TEM, Philips 208 S Morgagni, FEI, Czech Republic) at an accelerating voltage of 80 kV by scanning electron microscopy (SEM, Magellan 400L, FEI, Czech Republic). Size and polydispersity were determined using Multi-Angle Dynamic Light Scattering (MADLS) (Zetasizer Nano ZSP, Malvern, UK). Approximately 50 µL of the sample was placed in a low-volume quartz batch cuvette ZEN2112 (Malvern Panalytical Ltd., Malvern, UK) and measured using the MADLS® technique with a Zetasizer Ultra (Malvern Panalytical Ltd., UK) at a constant temperature of 25°C. The device was equipped with an HeNe Laser (633 nm) and three detectors at 173° (backscatter), 90° (side scatter), and 13° (forward scatter). Measurements were performed using a 10-fold dilutions of stock solutions in Milli-Q water and cell culture medium containing 10% autologous serum.

The zeta (ζ) potential of the analyte was determined by Electrophoretic Light Scattering (Zetasizer Nano ZSP, UK). Approximately 800 µL of each sample was placed in a folded capillary zeta cell DTS1070 (Malvern Panalytical Ltd., Malvern, UK). Analysis was performed at a constant temperature of 25°C in the monomodal mode. The data were evaluated using ZS Xplorer software version 3.50 (Malvern Panalytical Ltd, UK). The measured values are reported as mean ± standard deviation (n = 3).

Biological Contamination

Freshly prepared TiO_2 stock solution was checked for the presence of LPS using the Pierce™ Chromogenic Endotoxin Quant Kit (Thermo Fisher Scientific, USA) according to the manufacturer's protocol. The presence of active TLR4 and TLR2 agonists was assessed using HEK-Blue™-4 and HEK-Blue™-2 reporter cells (InvivoGen, USA), respectively, that stably express human TLR4 and TLR2. The fusion of the inserted secreted alkaline phosphatase (SEAP) gene with the nuclear factor kappa-light-chain-enhancer of activated B (NF-κB) transcription factor leads to dose-dependent AP secretion, which is measured in cell supernatants using the color-changing medium QUANTI-Blue™ (InvivoGen, USA).

Both cell lines were cultured (37°C, 5% CO_2) in Dulbecco's modified Eagle's high glucose medium without phenol red (DMEM; Corning, USA) supplemented with 10% heat-inactivated ultra-low endotoxin fetal bovine serum (FBS_{LE}; Biosera, France), 2 mM L-alanyl-L-glutamine (GlutaMAX; Life Technologies, USA), Normocin (100 µg/mL; InvivoGen, USA) and selective antibiotics 250X HEK-Blue™ Selection (InvivoGen, San Diego, CA, USA). For the experiments, cells were seeded in flat-bottom 96-well plates at a density of 5×10^4 cells per well and were treated overnight with the subtoxic level of TiO_2 (100 µg/mL). Ultrapure LPS from Escherichia coli K12 (0.01 µg/mL. InvivoGen, USA) and heat-killed Staphylococcus aureus (HKSA, 10^7 cells/mL, InvivoGen, USA) were used as controls. The supernatant (20 µL) was transferred to 180 µL of QUANTI-Blue™, and the absorbance was measured using a Synergy HTX microplate reader (Biotek, Germany) at a wavelength of 630 nm.

Cell Culture and Exposure to TiO_2

Isolation of Human Primary Monocytes

Isolation of monocytes from blood samples was performed under sterile conditions. Each donor sample (n=6) was processed separately. Approximately 50 mL of fresh peripheral blood was collected into EDTA-treated BD Vacutainer® tubes (Becton Dickinson, USA) and processed as follows. Blood samples were mixed with beads (pluriSpin® Human Monocyte Enrichment, pluriSelect Life Science, Germany) at a ratio of 50 µL beads to 1 mL blood and incubated for 20 min at room temperature. The samples were then diluted with PBS (1:1) and layered over Histopaque®-1077 (Sigma-Aldrich, USA) and centrifuged at 800 g for 15 min, with the brake turned off. Cells at the interface were collected and washed several times with PBS by centrifugation at 300g for 10 min. Erythrocytes were lysed for 10 min using a lysis solution containing 150 mM NH_4Cl. All procedures were performed at room temperature. The purity of the isolated monocytes was assessed using a Navios flow cytometer (Beckman Coulter, USA). Unless otherwise stated, the following experiments were conducted for each donor individually, and all treatments and controls were performed in triplicate or duplicate.

Co-Exposure Model

Freshly isolated monocytes were suspended in Roswell Park Memorial Institute (RPMI) 1640 without phenol red (Corning, NY, USA), supplemented with 10% human autologous serum, 2 mM GlutaMAX, and Primocin™ (100 μg/mL), seeded at 1×10^6/mL in a 96-well plate (0.18 mL), and allowed to adhere for 1 h at 37°C and 5% CO_2. The medium and non-adherent cells were removed and replaced with fresh medium containing TiO_2 (30–120 μg/mL), muramyl dipeptide MDP (5 μg/mL, InvivoGen, USA), ultrapure LPS (0.1 μg/mL), or their mixtures in a final volume of 0.2 mL. Untreated cells were used as negative controls. Cells treated with MDP or LPS alone were used as the controls. Specific inhibitors, MCC950 (10 μM; InvivoGen, USA) and GSK717 (5 μM; Sigma-Aldrich, USA), were used to verify the activity of NLRP3 and NOD2, respectively. After 24 h of incubation at 37°C and 5% CO_2, supernatants were collected for cytokine production and viability analysis.

Post-Exposure Model and Differentiation

Monocytes were seeded in a 96-well plate and incubated overnight at 37°C and 5% CO_2 with or without TiO_2 (120 μg/mL). To evaluate the activity of cAMP response element-binding protein (CREB), the inhibitor 666–15 (5 μM; Sigma-Aldrich, USA) was added. All cells were then carefully washed with RPMI 1640 to remove unincorporated TiO_2 and separately treated with MDP (5 μg/mL) or LPS (0.1 μg/mL) for another 24 h. Cells without pretreatment with TiO_2 were used as controls.

For the differentiation, freshly isolated monocytes were seeded at 2×10^6/mL in a 12-well plate (1 mL) and were allowed to adhere for 1 h at 37°C and 5% CO2. The medium and non-adherent cells were removed and replaced with fresh medium with or without TiO_2 (120 μg/mL). Following overnight incubation, the medium was replaced with complete medium without any treatment, and the cells were allowed to differentiate for another 11 days, with medium changes every 3 days. Cells without TiO_2 pretreatment were used as controls.

Viability Assessment

Cell viability was assessed using a lactate dehydrogenase (LDH) assay (CyQUANT™ LDH Cytotoxicity Assay, Thermo Fisher Scientific, USA) according to the manufacturer's protocol. The absorbance was measured using a Synergy HTX microplate reader at 490 nm, with the reference wavelength set at 690 nm. % Cytotoxicity was calculated according to absorbance values using the following formula:

$$\% = \left(\frac{\text{Treated cells} - \text{Untreated cells(negative control)}}{\text{Lysed cells} - \text{Untreated cells(negative control)}} \right) \times 100$$

Mitochondrial dehydrogenase activity was evaluated using a WST-1 assay. After removing the supernatant, a fresh complete medium containing 5% WST-1 reagent was added to each well. Cells were measured immediately and after 1 h of incubation (37°C, 5% CO_2) using a Synergy HTX microplate reader at 450 nm, with 650 nm set as the reference wavelength. The final absorbance was obtained by subtracting the values at time 0 from the values at time 1h, and results were expressed as the percentage of total cellular dehydrogenase activity relative to that in untreated cells (negative control = 100%).

Flow Cytometry

Flow cytometry was used to evaluate phenotypic changes in the cultured monocytes and differentiated macrophages. Cells were carefully detached using a cell scraper, washed with PBS containing 1 mM EDTA, 1% bovine serum albumin (BSA), 2% FBS_{LE}, and 0.1% sodium azide (NaN_3), and stained with respective antibodies. The monoclonal antibodies used for flow cytometry were purchased from three different companies. CD16 FITC, PC7 (clone 3G8), CD45 APC, KO (clone J33), CD14 ECD (clone RHO52), and CD64 PE (clone 22) were purchased from Beckman Coulter (USA). CD209 PerCP-Cy5.5 (clone 9E9A8), CD14 APC-Cy7 (clone M5E2), CD206 APC-Cy7 (clone 15–2), and CD86 BV510 (clone IT2.2) were purchased from BioLegend (USA). CD163 FITC (clone M130) was purchased from Trillium Diagnostics (USA). Flow cytometric data were acquired using Navios and NaviosEx (Beckman Coulter, USA) and analyzed using FlowJo V10 software (Becton Dickinson, USA). The gating strategies are provided in the Supplementary Materials.

Transmission Electron Microscopy

Monocytes exposed to TiO_2 for 24 h were carefully detached by cell scraper and fixed using 3% glutaraldehyde. The centrifuged pellet was rinsed in Milonig buffer, post-fixed in 1% OsO_4 solution in Milonig buffer, dehydrated in 50%, 70%, 90%, and 100% ethanol, embedded in Epon-Durcupan mixture (Epon 812 Serva, Heidelberg, Germany; Durcupan, ACM Fluka, Buchs, Switzerland), and polymerized at 60°C for 72 h. Ultrathin sections (60 nm) were cut with glass knives on UC 7 ultramicrotome (UC 7, Leica, Vienna, Austria) and contrasted with 2% uranyl acetate and 2% lead citrate. The obtained sections were observed using TEM (Philips 208 S Morgagni, FEI, San Jose, CA, USA).

NF-κB Reporter Assay

NF-κB activity was evaluated using RAW-Blue™ reporter cells (San Diego, CA, USA), which express a variety of pattern recognition receptors (PRRs) including TLR4 and NOD2. Stimulation of these receptors activates Nf-kB/AP-1 fused to SEAP. The resulting AP production was detected using QUANTI-Blue™. RAW-Blue™ were cultured in DMEM supplemented with 10% heat-inactivated FBS_{LE}, 2 mM GlutaMAX, Normocin (100 μg/mL), and selective antibiotics Zeocin®. Cells were maintained at 37°C in a humidified atmosphere containing 5% CO_2 and handled according to the manufacturer's instructions. For the experiment, cells were seeded in a flat-bottom 96-well plate at a density of 10^5 cells/well and incubated overnight at 37°C and 5% CO_2 with TiO_2 (120 μg/mL), MDP (5 μg/mL), ultrapure LPS (0.1 μg/mL), or their mixtures in a final volume of 0.2 mL. Each treatment and control were performed in triplicate. The absorbance was measured using a Synergy HTX microplate reader (Biotek, Germany) at a wavelength of 630 nm.

NLRP3 Reporter Assay

Canonical activation of NLRP3 was evaluated using THP1-null cells (San Diego, CA, USA), a positive control cell line with high expression of NLRP3, apoptosis speck-like protein (ASC) and pro-caspase-1. Cells were cultured at 37°C in a 5% CO2 in RPMI1640 without phenol red supplemented with 10% heat-inactivated FBS_{LE}; 2 mM GlutaMAX, Normocin (100 μg/mL), 25 mM HEPES (Sigma-Aldrich, USA), 1 mM sodium pyruvate (Life Technologies, USA), Normocin (100 μg/mL) and selection antibiotic Hygromycin B Gold (200 μg/mL; InvivoGen, USA).

For experiments, cells were seeded in the 96-well plate at 1.8×10^5 cells per well and activated by phorbol 12-myristate 12-acetate (PMA; 30 ng/mL, Sigma-Aldrich, USA) for 3 h. After removing PMA, they were left to attach and differentiate for another 72 h in fresh complete medium at 37°C in a 5% CO2. Cells were further primed with ultrapure LPS (1 μg/mL, 3 h) or left unprimed and after washing exposed to TiO_2 (10–120 μg/mL), muramyl dipeptide MDP (5 μg/mL), or their mixtures in fresh medium of a final volume of 0.2 mL. Untreated cells (primed or unprimed) were used as negative controls. Cells treated with MDP alone were used as the controls. Nigericin (1 μM, InvivoGen, USA) was used as a positive control. Specific inhibitors, MCC950, GSK717 and A151 (10 μM; InvivoGen, USA), were used to verify the activity of NLRP3, NOD2 and AIM2, respectively. Each treatment was performed in triplicate. After 24 h of incubation at 37°C and 5% CO2, supernatants were collected for cytokine production and LDH assay. Dehydrogenase activity was assessed using WST-1 assay.

Cytokines Measurements

Bioactive IL-1β and IL-10 Measurements

IL-10 and IL-1β released by monocytes and IL-1β released by THP1-null were detected using HEK-Blue™ IL-1β and HEK-Blue™ IL-10 reporter cells (San Diego, CA, USA) according to the manufacturer's instructions. The specific response of these cells is ensured by the endogenous expression of their respective receptors, whose binding cytokines lead to the activation of their respective transcription factors fused to SEAP. HEK-Blue cells were cultured in DMEM supplemented with 10% heat-inactivated FBS_{LE}, 2 mM GlutaMAX, Normocin (100 μg/mL), and selective antibiotics Zeocin® and Hygromycin B. Cells were maintained at 37°C in a humidified atmosphere containing 5% CO_2 and handled according to the manufacturer's instructions. For experiments, cells were seeded in a 96-well plate at 5×10^4 cells per well. Fifty microliters of supernatant from examined monocytes were added, and the samples in a final volume of 0.2 mL

were incubated overnight at 37°C in a 5% CO_2. The supernatant (50 µL) was then transferred to 150 µL of QUANTI-Blue™ and the absorbance was measured using a Synergy HTX microplate reader at a wavelength of 630 nm.

ELISA

IL-10 levels were also determined using the Invitrogen Human IL-10 Uncoated ELISA Kit (Thermo Fisher Scientific, USA) according to the manufacturer's protocol. The samples were diluted 2-fold. The detection range was 2–300 pg/mL. Absorbance was measured at a wavelength of 450 nm using a Synergy HTX microplate reader, with the reference wavelength set at 570 nm.

Statistical Analysis

Data from all experiments were obtained from at least three independent experiments (from different donors), performed in duplicate or triplicate. The analysis was performed using GraphPad Prism™ version 8.2.1 (GraphPad Software Inc., CA, USA). Based on the Shapiro–Wilk normality test and analysis of variance (F-test), either parametric or nonparametric analysis of variance (ANOVA) or Brown-Forsythe and Welch's test followed by Dunnett's test or Kruskal–Wallis's post hoc tests were performed. The Sidak correction was used for multiple comparisons. In the case of phenotypic changes in monocytes and macrophages and ELISA assays, the results were evaluated separately using a paired *t*-test or Wilcoxon test. Statistical significance was determined based on the p-values of * $p<0.05$, ** $p<0.01$, and *** $p<0.001$.

Ethics

This study was conducted in accordance with the Declaration of Helsinki guidelines. Peripheral blood samples were obtained from healthy volunteers (6 donors) after obtaining their consent and approval from the Ethics Committee of the University Hospital Hradec Kralove, Sokolska 581, 50005 hradec Kralove (reference number 202209 P05), Czech Republic.

Results

TiO_2 Characterization

The physicochemical characterization of TiO_2 used in this study has been described in detail in the study of Bacova et al.[30] The basic characteristics of TiO_2 dispersed in water and full medium containing 10% autologous serum are shown in Table 1. TEM and SEM images and DLS confirmed the presence of aggregates (Figure 1A–C). The size of the primary particles was 30 ± 10 nm, following the manufacturer's information (Figure 1A).

Endotoxin levels evaluated using the LAL assay were < 0.1 EU/mL. The absence of TLR4 and TLR2 agonists was confirmed using the HEK-Blue™-4 and HEK-Blue™-2 reporter cell lines (Figure 1D).

TiO_2 Uptake by Human Primary Monocytes

The intracellular localization of TiO_2 and morphology of the treated monocytes were examined using TEM. After 24 h of incubation, the TiO2 nanoparticles were mostly sequestered as aggregates across the cytoplasm (Figure 2A). The presence of TiO_2 in membrane-bound compartments indicated active endocytosis (Figure 2B). Free particles without clear binding to the organelles were also observed. No particles reached the nucleus.

Table 1 Characterization of TiO_2 in DI Water and Full Medium (RPMI, 10% Autologous Serum)

Vehicle	Z-Average (nm)	PdI	Average ζ-Potential (mV)
Water	151 ± 7	0.145 ± 0.021	21 ± 0.64
Full medium	270 ± 9	0.21 ± 0.006	−9.06 ± 1.13

Abbreviation: PdI, polydispersity index.

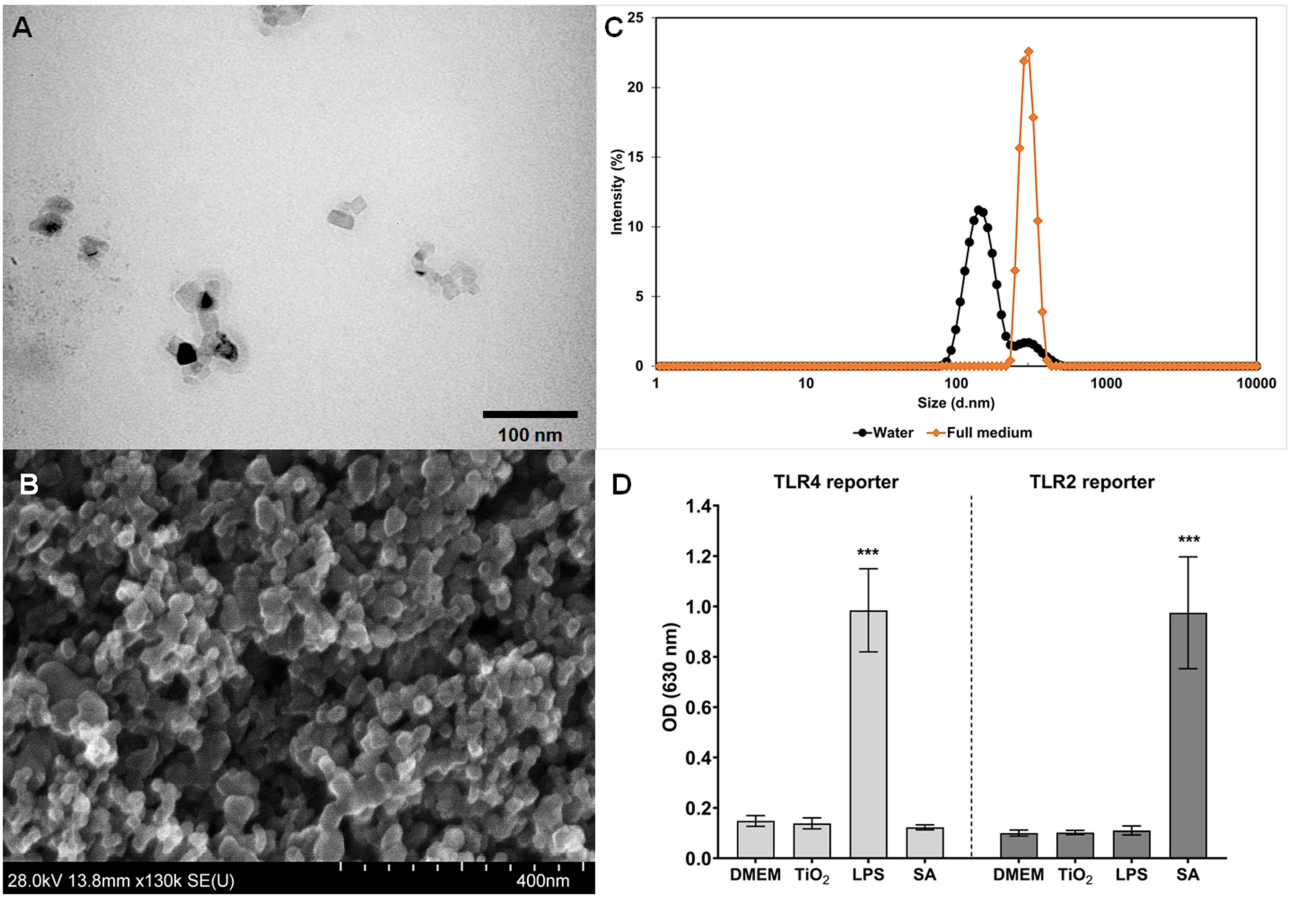

Figure 1 Characterization of TiO_2.
Notes: (**A**) TEM image of TiO_2 individual particles; (**B**) SEM image of TiO_2 forming aggregates; (**C**) average size distribution measured by dynamic light scattering in distilled water and full medium containing 10% autologous serum; (**D**) Evaluation of biological contamination of the TiO_2 nanoparticles using HEK-Blue™-4 and HEK-Blue™-2 reporter cells. Data are presented as mean of three independent experiments with ± SD. *** $p < 0.001$ highlights statistical significance as compared to untreated control (DMEM).
Abbreviations: TEM, transmission electron microscopy; LPS, Lipopolysaccharide; SA, *Staphylococcus aureus*; TLR, Toll-like receptor.

The effect of endocytosed TiO_2 on monocytes was further investigated by examining the CD14/CD16 phenotype using flow cytometry (Figure 2C). Before treatment, freshly isolated monocytes were mostly composed of the $CD14^{++}/CD16^{+}$ cells (~ 78%, Figure S1). After 24 h of incubation, the number of $CD14^{++}/CD16^{+}$ monocytes was reduced both in untreated control and TiO_2–loaded monocytes. Nevertheless, the number of TiO_2–loaded $CD14^{++}/CD16^{+}$ monocytes was significantly higher than that of the control (Figures 2D and S2). Approximately 50% of control monocytes were formed from $CD14^{+}/CD16^{\pm}$ subset, which was on the contrary significantly reduced (~15%) in the case of TiO_2-loaded monocytes. The remaining cells were composed of the $CD14^{++}/CD16^{++}$ and $CD14^{+}/CD16^{+++}$ subsets, with an apparent shift towards high expression of CD16, but no significant differences were observed between the untreated control and TiO_2 monocytes.

Costimulatory Effects of TiO_2 on NLRP3 Assembly

According to the results of the WST-1 and LDH assays, TiO_2 nanoparticles alone (dose range, 30–120 μg/mL) did not cause any acute cytotoxic reactions (Figure 3A and B). Similar results were observed in experiments evaluating the impact of TiO_2 (dose range, 10–120 μg/mL) on THP1-null cells (Figure S3A and B). Moreover, TiO_2 alone did not induce substantial release of the proinflammatory cytokines IL-1β, IL-6, and TNF-α, or the regulatory cytokine IL-10 (Figures 3C, D, S3C and S4A). The absence of elevated levels of IL-6, TNF-α, and IL-10 was verified using ELISA (Figure S4B).

https://doi.org/10.2147/IJN.S498690

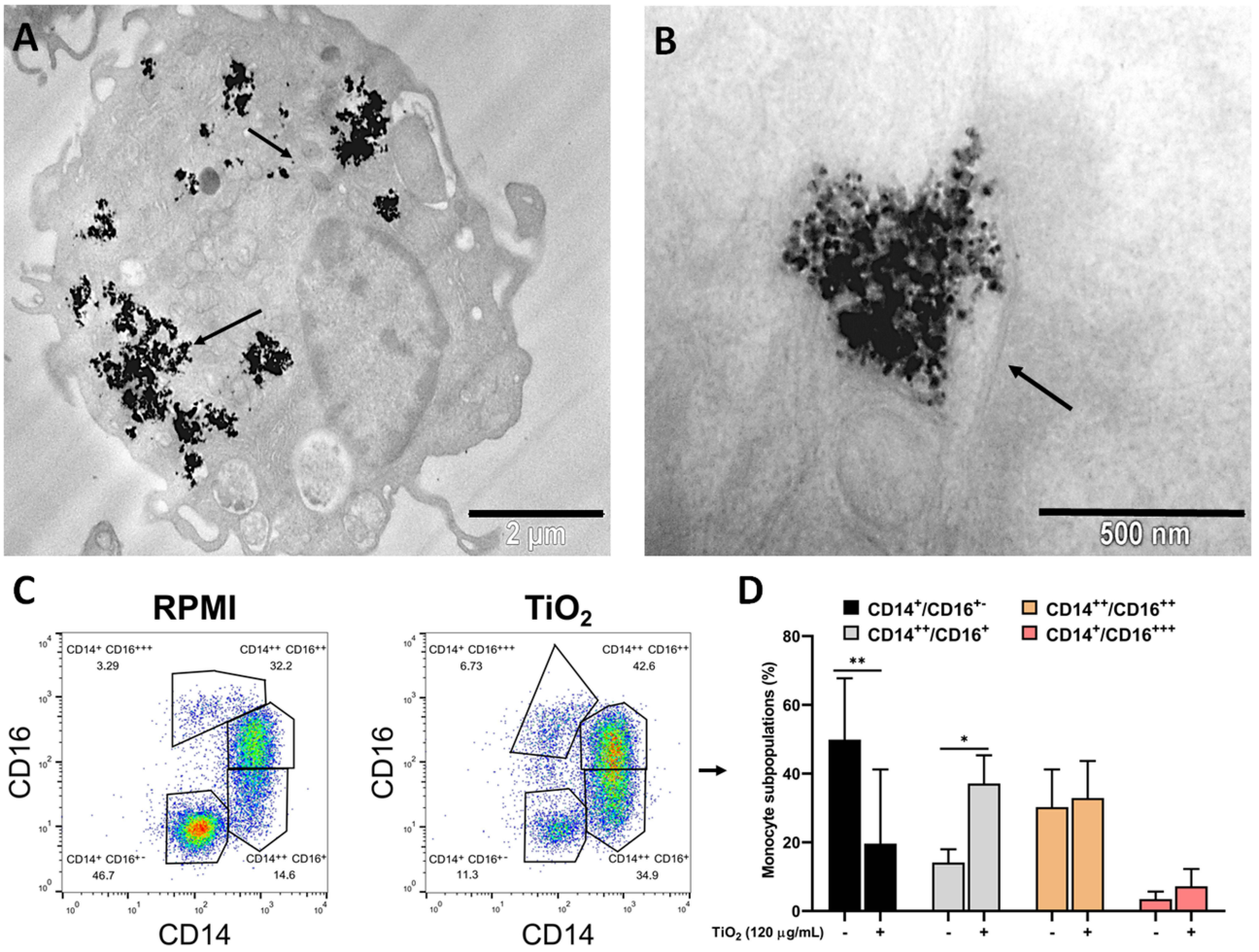

Figure 2 Morphology and phenotype of monocytes after 24 h incubation with TiO_2.

Notes: (**A**) TEM image of intracellular distribution of TiO_2 (arrows); scale bar = 2 µm; (**B**) TEM image with detail of TiO_2 forming aggregate surrounded by double membrane (arrow), scale bar = 500 nm; (**C**) Representative flow cytometry analysis of CD14 and CD16 expression on monocytes after 24 h of incubation with TiO_2 and untreated monocytes (RPMI), (**D**) The comparison of CD14/CD16 subsets between TiO_2 monocytes and untreated control. Data of three independent experiments/donors are presented as the mean ± SEM with ** $p < 0.01$, * $p < 0.05$, highlighting statistical significance compared to the corresponding control within each subset (n = 3, Paired *t*-test).

Abbreviations: TEM, transmission electron microscopy; CD, cluster of differentiation; SEM, standard error of the mean.

To further investigate the potential immunomodulatory effects of TiO_2, monocytes were costimulated with TiO_2 in the presence of the typical proinflammatory stimuli LPS (0.1 µg/mL) or MDP (5 µg/mL). We focused on inflammasome activation and subsequent IL-1β release, as this has been described as a key effector mechanism of engineered nanoparticle immunotoxicity. As expected, both LPS and MDP induced mild IL-1β production and increased dehydrogenase activity (Figure 3B and C). However, the production changed substantially in the presence of TiO_2.

Co-exposure of monocytes to MDP and TiO_2 augmented IL-1β release without affecting cell viability. The cytokine response was dose-dependent, with significance observed at the highest tested dose (120 µg/mL). The exclusive role of NLRP3 inflammasome assembly was confirmed by the complete inhibition of IL-1β release in the presence of the NLRP3 inhibitor MCC950 (10 µM) (Figure 4A). Interestingly, the NOD2 inhibitor GSK717 (5 µM) had only a moderate effect on IL-1β production stimulated by both MDP and a mixture of MDP/TiO_2.

To characterize the found co-stimulatory effect, additional experiments were conducted using MDP (5 µg/mL) as a "priming" before TiO_2 stimulation. The results showed that 1 h of monocyte priming with MDP led to increased production of IL-1β after 24 h of exposure to TiO_2 (Figure S5). Thus, the IL-1β response of monocytes to a mixture of MDP and TiO_2 was assumed to be based on canonical NLRP3 activation, which usually requires two signals. Both the alternative and canonical pathways of NLRP3 assembly involve the activation of NF-κB, but only the alternative

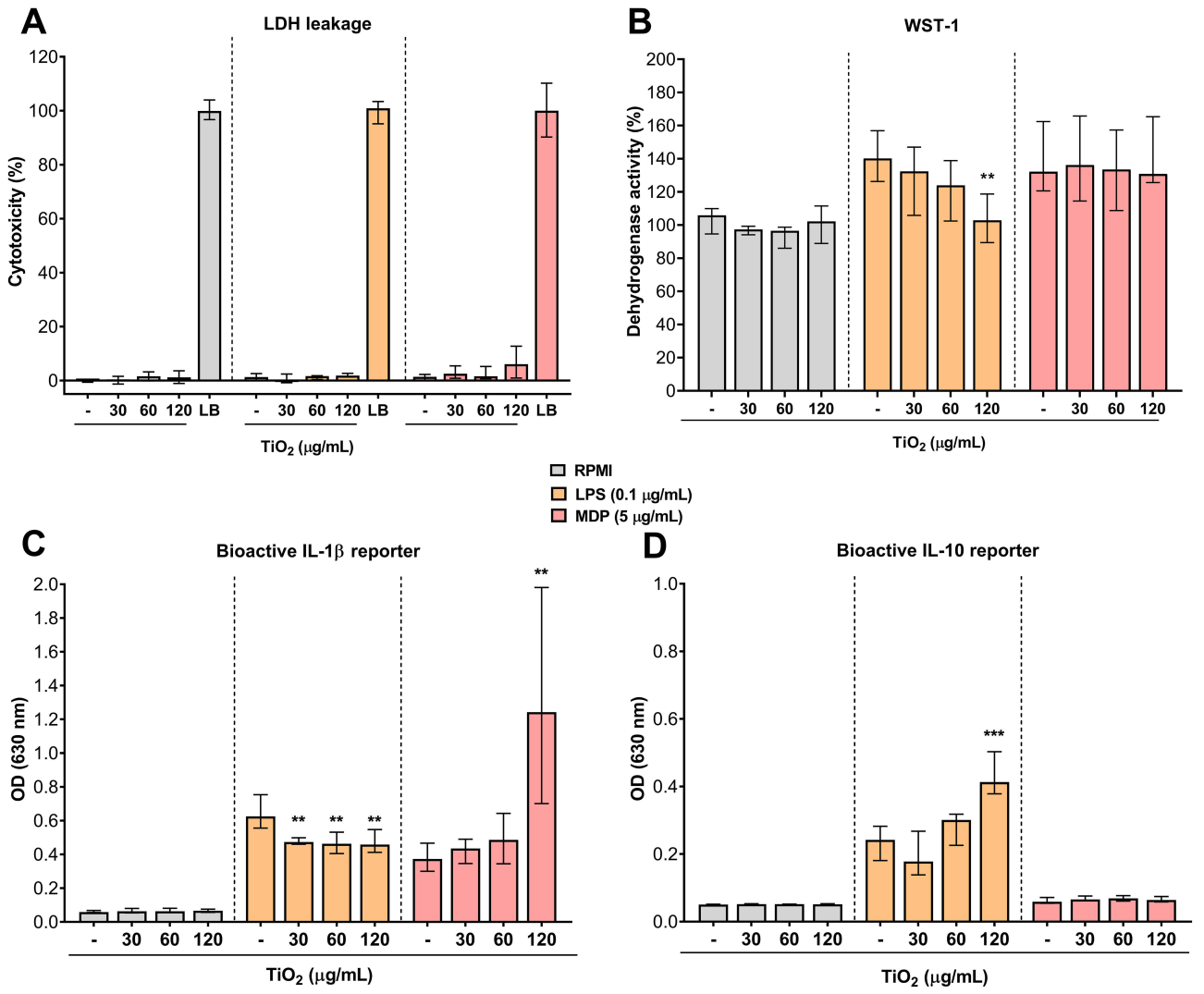

Figure 3 Viability and cytokine response of human primary monocytes in co-exposure model.

Notes: For 24 h, cells were incubated with either TiO_2 alone or in the presence of NOD2 and TLR4 agonists MDP and LPS, respectively, viability was assessed by (**A**) LDH assay with lysis buffer as 100% positive control and (**B**) WST-1 assay. Results were obtained from three independent experiments/donors with three replicates of each, n = 9, (**C**) IL-1β and (**D**) IL-10 production were evaluated using reporter cell-based assays. Results were obtained from four independent experiments/donors with triplicate of each, n = 12. All data were analyzed separately for each corresponding control without TiO_2 treatment (RPMI, LPS, and MDP) and are reported as medians with interquartile ranges. *** $p < 0.001$, ** $p < 0.01$.

Abbreviations: NOD2, nucleotide oligomerization domain 2; TLR4, Toll-like receptor 4; LDH, lactate dehydrogenase; WST-1, water-soluble tetrazolium salt; LB, lysis buffer; IL, interleukin; LPS, lipopolysaccharide; MDP, muramyl dipeptide.

pathway of NLRP3 is fully activated. Therefore, the effect of TiO_2 on NF-κB was evaluated using a RAW-blue reporter cell line. Figure 4B shows that TiO_2 at the highest dose tested (120 μg/mL) neither activated nor inhibited NF-κB. There was also no significant synergistic effect on NF-κB when RAW-Blue cells were co-exposed to TiO_2, MDP, and LPS.

The role of TiO_2 in the canonical activation of NLRP3 was also confirmed in separate experiments using THP1-null cells, a positive control cell line, where TiO_2 failed to activate NLRP3 without priming (Figure S3C). Furthermore, co-exposure to MDP also did not induce significant levels of IL-1β. Without affecting viability (Figure S6A and B), the co-inducing effect of MDP was only apparent after 3h priming of THP1-null cells with LPS (Figure S6C), suggesting the need for significantly stronger stimuli than in the case of primary monocytes. Nevertheless, the absence of pyroptosis and the specific inhibition of NLRP3 (Figure S6D) corresponded with previous findings.

In contrast to MDP, LPS-induced IL-1β release from monocytes was reduced over the entire range of TiO_2 concentrations tested (Figure 3C). Moreover, there was a dose-dependent decrease in dehydrogenase activity compared

https://doi.org/10.2147/IJN.S498690

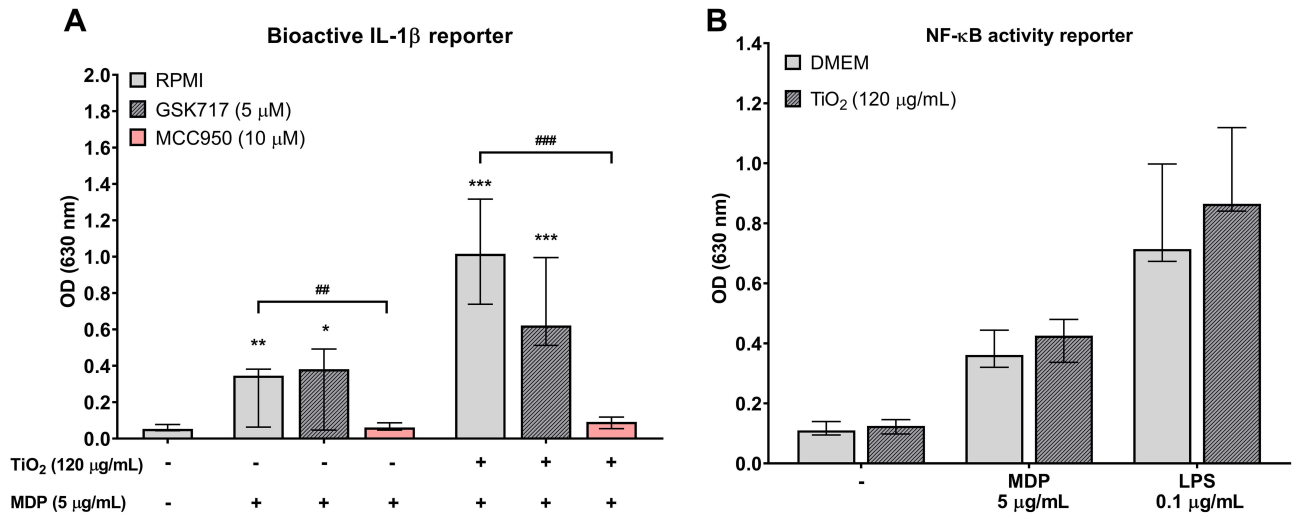

Figure 4 Estimation of TiO_2 costimulatory effect on specific NLRP3 activity.
Notes: (**A**) Cells were exposed to TiO_2, MDP, or their mixture for 24 h in the presence of the NOD2 and NLRP3 inhibitors GSK717 and MCC950, respectively. Data were obtained from three independent experiments/donors with three replicates of each, n = 9 and are reported as median with interquartile range with *** $p < 0.001$, ** $p < 0.01$, and * $p < 0.05$, highlighting statistical significance compared to the unstimulated control (RPMI), and $^{\#\#}p < 0.01$, $^{\#\#\#}p < 0.001$ highlighting statistical significance compared to the stimulated control without inhibitor. (**B**) NF-κB activity was assessed using reporter HEK-Blue™ cells that were exposed to TiO_2, MDP, LPS, or their mixtures for 24 h. Data are reported as medians of three independent experiments (n = 9) with interquartile ranges.
Abbreviations: NOD2, nucleotide oligomerization domain 2; NLRP, nucleotide-binding oligomerization domain; leucine-rich repeat and pyrin domain containing; NF-κB, Nuclear factor kappa-light-chain-enhancer of activated B cells; LPS, lipopolysaccharide; MDP, muramyl dipeptide.

with that observed with LPS alone (Figure 3B). Nevertheless, another cytokine analysis revealed a significant costimulatory effect on LPS-based IL-10 production (Figure 3D). The same effect was absent from MDP-TiO_2 treatment, suggesting a possible mechanism for IL-1β inhibition by IL-10 augmentation.

Inhibition of NLRP3 Activity by Augmentation of IL-10 Production

To avoid the Trojan horse effect in the modulatory role of TiO_2 and to explore the dynamics between IL-1β and IL-10 cytokine production, monocytes were first pretreated with TiO_2 alone (1st stim, 120 μg/mL). After removing the unincorporated nanoparticles, the cells were further treated with LPS (0.1 μg/mL) or MDP (5 μg/mL) (2nd stim). Additional pretreatment with MDP and MDP-TiO_2 was included as a model of acute inflammation. Figure 5A shows that the already incorporated TiO_2 had no effect on MDP-based IL-1β production but induced IL-10 production, which was previously absent (Figure 3D). However, the concentration of IL-10 was below the detection limit of the cell-based assay, and the results were only detectable by ELISA. Nevertheless, despite biological inter-individual variability, the increased level of IL-10 was apparent for all donors (Figure 5A). More prominent data were obtained when LPS was used as the secondary stimulus. Figure 5B shows that pretreatment of monocytes with TiO_2 resulted in significantly higher production of IL-10 in response to LPS than in the case of monocytes without previous TiO_2 treatment. Consistent with the data from the costimulation model, IL-1β production was, on the contrary, decreased. The same effect was observed when monocytes were pretreated with the MDP or MDP-TiO2 mixture as an inflammatory model. Although pretreatment with MDP alone enhanced LPS-based IL-1β release, the presence of TiO_2 reduced this production and enhanced IL-10 production (Figure 5B).

Additional experiments showed that there was a slight increase in LDH leakage after the pretreatment with the CREB inhibitor 666–15, but at the margin of significance (Figure 6A). The subsequent LPS-induced IL-10 production was completely blocked (Figure 6B). However, LPS treatment had no further effect on cell viability (Figure 6C). Owing to high variability, we could not verify the effect of 666–15 on IL-1β levels.

Differentiation of TiO_2 Pretreated Monocytes to Macrophages

Previous results suggested that TiO_2 incorporation preferentially modulated the inflammatory response of monocytes in a regulatory manner. For this reason, we investigated whether the initial encounter with TiO_2 influences monocytes in the

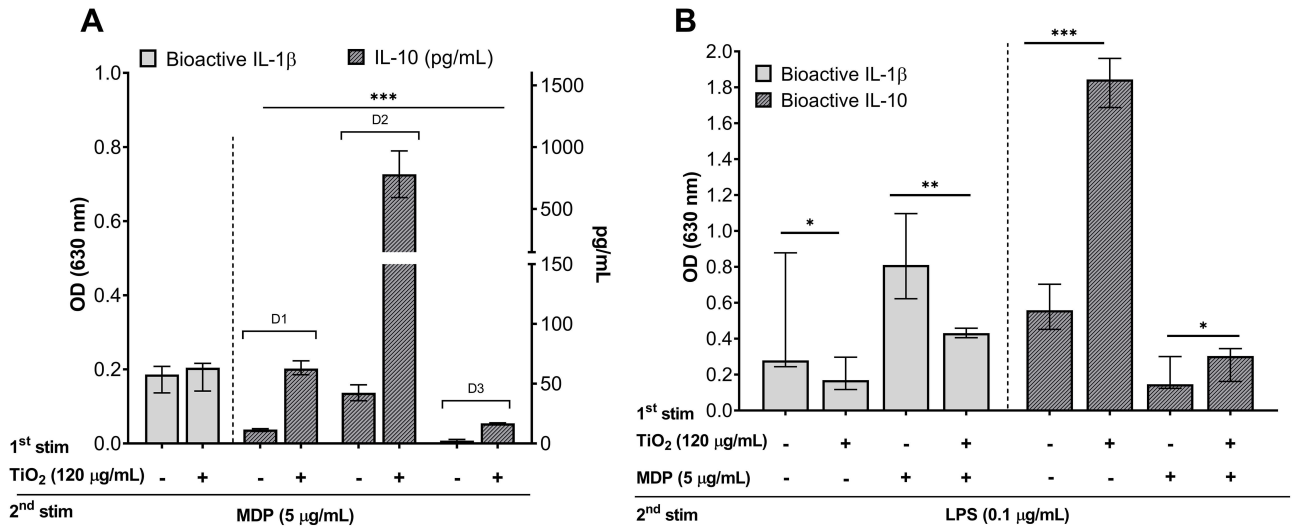

Figure 5 Cytokine response of human primary monocytes in post-exposure model.
Notes: (**A**) Cells were incubated overnight in full medium with or without TiO_2 (1^{st} stim). After washing, the cells were re-stimulated with MDP for 24 h (2^{nd} stim) Results were obtained from three independent experiments/donors with three replicates of each, n = 9. (**B**) Cells were incubated overnight in full medium with or without TiO_2 (1^{st} stim), MDP, or TiO_2-MDP mixture (1^{st} stim). After washing, the cells were re-stimulated with LPS for 24 h (2^{nd} stim). The results of subsequent cytokine production were obtained from three independent experiments with three replicates of each, n = 9. Results of IL-10 (**A**) production are presented individually for each independent experiment (donor) separately with three replicates of each (n = 9, paired Wilcoxon test). All data are reported as medians with interquartile ranges. *** $p < 0.001$, ** $p < 0.01$ and * $p < 0.05$ highlight statistical significance as compared to the corresponding control without initial TiO_2 treatment.
Abbreviations: IL, interleukin; LPS, lipopolysaccharide; MDP, muramyl dipeptide; D, donor.

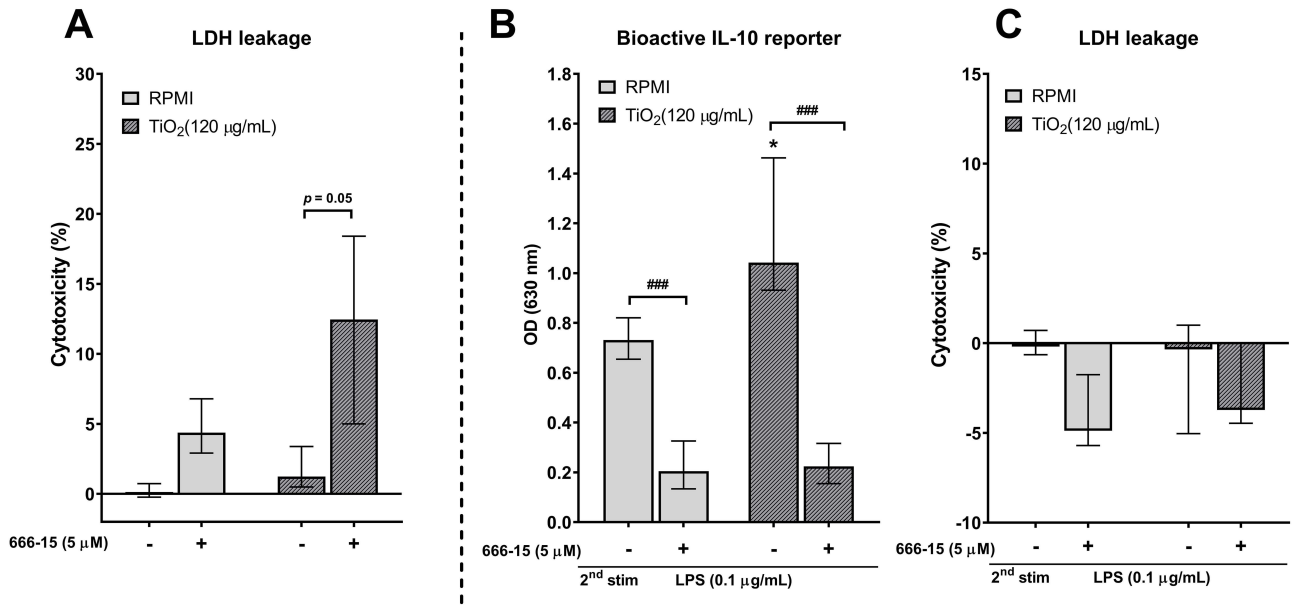

Figure 6 Effect of CREB inhibitor 666–15 on LPS-induced IL-10 production.
Notes: Cells were incubated overnight in full medium with or without TiO_2 (1^{st} stim) in the presence or absence of the CREB inhibitor 666–15. After washing, the cells were re-stimulated with MDP for 24 h (2^{nd} stim). (**A**) Monocyte viability was assessed using LDH assay (**A**) before and (**C**) after LPS treatment. (**B**) Evaluation of IL-10 production after LPS treatment. Results were obtained from three independent experiments/donors with two replicates of each, n = 6. Data are reported as median with interquartile range with * $p < 0.05$, highlighting statistical significance compared to the control without TiO_2 (RPMI) and $^{###}p < 0.001$, highlighting statistical significance compared to the corresponding control without inhibitor.
Abbreviations: CREB, cAMP response element binding protein; LDH, lactate dehydrogenase; LPS, lipopolysaccharide; MDP, muramyl dipeptide.

long term, presumably by shifting their differentiation towards anti-inflammatory macrophages. For this purpose, freshly isolated monocytes were incubated with TiO_2 (120 μg/mL) overnight and then washed carefully to remove unincorporated NPs. Unexposed cells served as a control. Both control and treated monocytes were allowed to differentiate in fresh medium for 11 days without additional TiO_2 treatment or any other stimulus. On day 12, macrophages were observed

https://doi.org/10.2147/IJN.S498690

under an optical microscope. As shown in Figure 7A, the number of control cells (RPMI) was reduced compared to TiO_2 treated cells, which were large with rounded shapes and remained well attached to the surface of the well plate. Microscopic analysis confirmed that initially ingested TiO_2 persisted within cells throughout the differentiation process.

The observed macrophages were then harvested, and their phenotype was assessed based on the expression of specific CD markers. Flow cytometry showed that both control and TiO_2-treated monocytes differentiated into heterogeneous populations consisting of two major subsets distinguished by the rate of CD14 expression (Figure 7B). Comparable in both control and TiO_2-treated cells, a subset with higher CD14 expression ($CD14^{high}$) prevailed (~ 65%). For some donors, a subset with high expression of CD16 was also present, however its representation was less than 1%; thus, was excluded from the final analysis.

Macrophage polarization was based on the M1 markers CD64 and CD86 and M2 markers CD163, CD206, and CD209 (Figure 7C). Within the $CD14^{high}$ macrophages, TiO_2 macrophages expressed CD64, CD163, CD206, and CD209 at a significantly higher rate than control macrophages (Figure 7D). Within the $CD14^{med}/CD16^{med}$ subset, the only significant difference was found in the expression of CD206, which, on the other hand, was decreased in TiO_2 macrophages. Analysis of the supernatants of both control and TiO_2 macrophages showed no measurable production of IL-10 or IL-1β (data not shown), suggesting resting state. Only additional treatment of differentiated TiO_2 macrophages with LPS induced a significant IL-10 release, but due to notably lower number of the control macrophages, the data could not be compared.

Discussion

Professional phagocytes, notably the mononuclear phagocyte system (MPS), are an essential tool for the recognition and processing of foreign particles. Several studies have confirmed that engineered nanoparticles are primarily processed by these cells.[16] The majority of studies have documented the effect of TiO_2 nanoparticles on macrophages or macrophage-like cells.[31,32,34–36,40] However, the effect of these nanoparticles on blood monocytes has been investigated to a significantly lesser extent.[41] Similar to macrophages, monocytes possess high phagocytic capacity and plasticity, which together with their differentiation potential, make them an ideal target for possible immunotoxic effects.[41,42] Because the underlying mechanism of immunotoxicity is dysregulated inflammation,[43] this study aimed to evaluate whether TiO_2 nanoparticles affect monocytes in their physiological inflammatory responses.

The first step of such response is the recognition and uptake of the nanoparticles.[44,45] In agreement with studies using macrophages, TEM analysis confirmed that primary monocytes efficiently ingested TiO_2 P25 nanoparticles (Figure 2A and B).[35] According to the flow cytometry analysis, this encounter caused a shift in the expression of main monocytic markers CD14 and CD16 (Figure 2C). Under physiological conditions, circulating monocytes predominantly express CD14 ($CD14^{++}/CD16^{+-}$ ~ 85%), forming a proinflammatory subset called classical monocytes. The rest of the monocytes form intermediate and non-classical (patrolling) subsets, $CD14^{+}/CD16^{+}$ and $CD14^{+-}/CD16^{++}$, respectively.[18,46] After isolation, monocytes cultivated in vitro without specific stimuli usually downregulate their CD14 expression.[42,47] This corresponds with our finding on control monocytes, which partially decreased their expression of CD14 after 24 h of cultivation (Figures 2C and S2). By contrast, TiO_2-treated monocytes maintained a high expression rate of CD14, mainly in the $CD14^{++}/CD16^{+}$ subset. Other minor subsets increased the expression of CD16, but there were no significant differences between control and TiO_2-treated monocytes (Figure 2C and D). In general, this "activation" might relate to a better survival rate of TiO_2-treated monocytes and their differentiation into macrophages,[48,49] which we also observed (Figure 7), as discussed below.

Despite previous results, we did not confirm a significant enhancement in the production of proinflammatory cytokines IL-6, TNF-α, and IL-1β (Figures 3C and S4) in response to TiO_2 nanoparticles alone. These results are consistent with the absence of biological contamination (Figure 1D). Moreover, no significant cytotoxicity was observed (Figure 3A and B), which was in accordance with results from separate experiments using THP1-null cells (Figure S3A and B). Nevertheless, our previous study on graphene platelets (GP) showed that although nanoparticles alone do not cause a direct proinflammatory reaction, they still affect the inflammatory response when co-cultured with bacterial compounds.[50] Some studies even emphasized the necessity of evaluating the toxicity of nanoparticles in the presence of a bacterial PAMP, especially in the field of nanotoxicology.[51,52] Thus, we evaluated the immunotoxic effect of TiO_2 in the

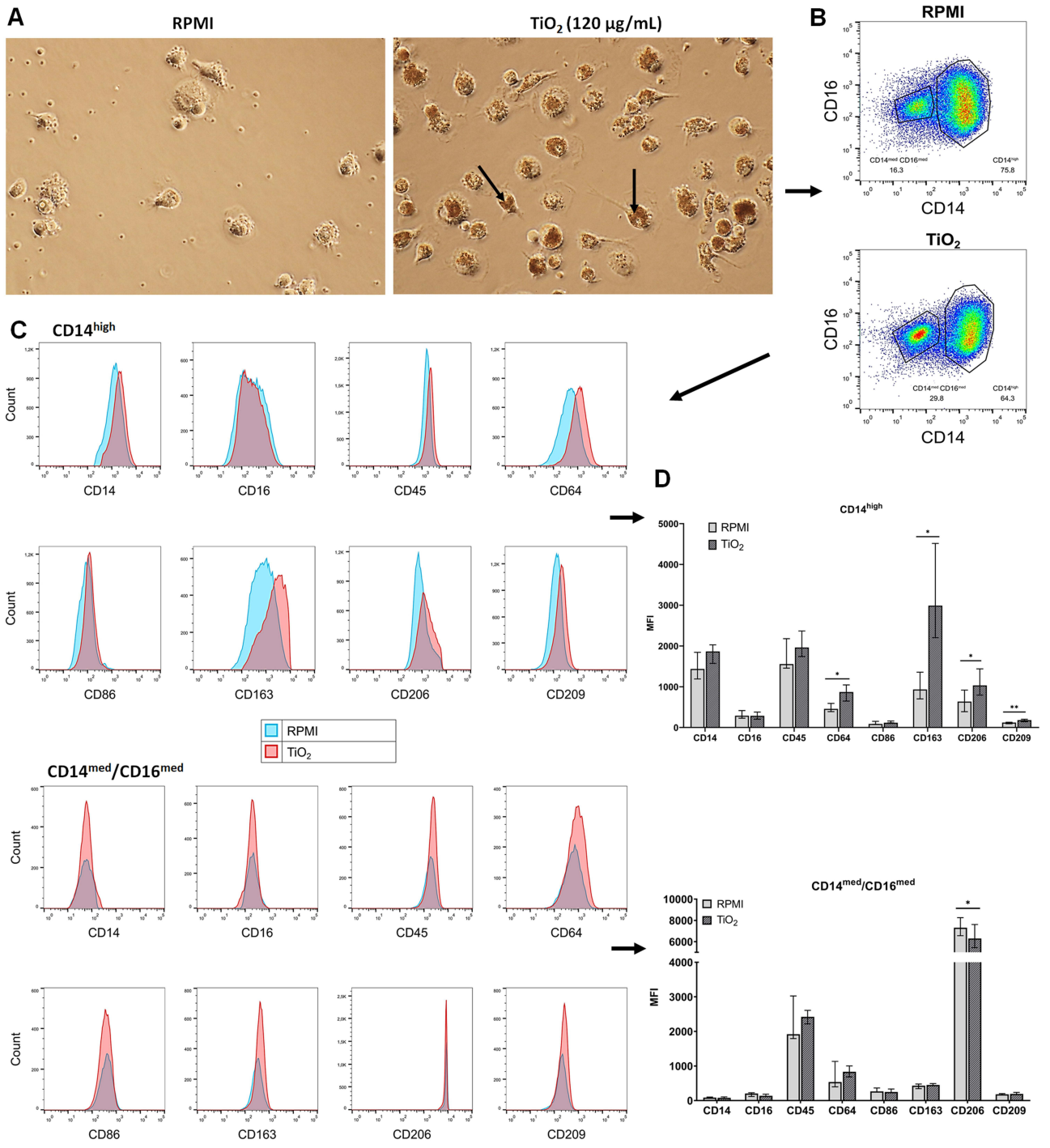

Figure 7 Morphology and phenotype of differentiated macrophages.

Notes: (**A**) Optical microscopy images of untreated cells (RPMI) and TiO_2 pretreated cells, magnification ×20; (**B**) Representative flow cytometry analysis of CD14 and CD16 expression in macrophages after 12 days of differentiation; (**C**) Flow cytometry analysis of M1 and M2 marker expression in two major macrophage subsets, $CD14^{high}$ and $CD14^{med}/CD16^{med}$. (**D**) Comparison of M1 and M2 markers between control and TiO_2 macrophages in two major macrophage subsets: $CD14^{high}$ and $CD14^{med}/CD16^{med}$. Data of four independent experiments/donors are expressed as median with interquartile range with ** $p < 0.01$, * $p < 0.05$, highlighting statistical significance compared to the corresponding control within each marker ($n = 4$, Paired *t*-test, paired Wilcoxon test).

Abbreviation: CD, cluster of differentiation.

presence of the proinflammatory inducers LPS and MDP, which are typical agonists of the TLR4 and NOD2 receptors, respectively. We focused on the activation of the NLRP3 inflammasome associated with the release of IL-1β, which has been described as an indispensable mechanism underlying the pro-inflammatory effect of engineered nanoparticles.[32,50,53–55] Similar to our previous study on GP,[50] co-exposure of monocytes to TiO_2 and MDP significantly

https://doi.org/10.2147/IJN.S498690

amplified IL-1β production compared to MDP alone (Figure 3C). The specific role of NLRP3 was confirmed using the selective inhibitor, MCC950. In addition, the complete blockade of IL-1β by MCC950, together with the negligible effect of the NOD2 inhibitor GSK717, suggested that the observed costimulatory effect was exclusive to NLRP3 (Figure 4A).

As previously mentioned, NLRP3 activation is typical for engineered nanoparticles, which also applies to TiO_2.[32,56,57] However, canonical activation of NLRP3, which is characteristic (but not exclusive) for macrophages, requires two signals. The first essential step is priming, which leads to the activation of the transcription factor NF-κB and subsequent synthesis of pro-caspase-1 and pro-IL-1β. The second signal usually originates from intracellular damage causing the production of DAMPs, which are recognized by NLRP3 and lead to its full assembly.[58] The potential of TiO_2 to activate NLRP3 canonically was verified by additional experiments using THP1-null-derived macrophages as positive control cells. In this case, the significant release of IL-1β was measured only in cells that had been primed with LPS (Figure S6C). In the case of primary monocytes, NF-κB is also associated with an alternative pathway that does not require a second stimulus and is induced directly, eg by activation of TLRs.[59,60] However in our study, TiO_2 alone did not stimulate either TLR2, TLR4, or NF-κB (Figures 1D and 4B), confirming that TiO_2 do not activate an alternative pathway. This is in an agreement with the work of Tsugita et al, who concluded that mere internalization of TiO_2 is not sufficient for the induction of inflammasome-based IL-1β secretion.[38]

On the other hand, TiO_2 P25 nanoparticles have been confirmed to cause diverse types of oxidative stress,[30,34,38,61] which may serve as a second stimulus in the NLRP3 canonical pathway.[62,63] Thus, we hypothesized that the costimulatory effect on MDP-TiO_2-induced NLRP3 on monocytes was based on the canonical pathway, where MDP served as priming. This was further supported by the increased IL-1β production in response to TiO_2 when monocytes were first pretreated with MDP for 1 and 3 h (Figure S5). MDP, as a part of peptidoglycans of most Gram-negative and Gram-positive bacteria, has been previously identified as an inducer of NOD2 through which it activates NF-κB.[64] Martinon et al also reported that MDP is sensed by NLRP3,[65] suggesting that it may serve as both the first and second stimuli in NLRP3 assembly. If we consider the activation of NF-κB through NOD2 stimulation, additional ROS induced by TiO_2 contribute to cellular stress, leading to a boost IL-1β production, confirming the ability of TiO_2 to activate NLRP3 via the canonical pathway.

Interestingly, the co-exposure to the same level of MDP and TiO_2 was not sufficient to augment IL-1β production from unprimed THP-1 null cells (Figure S3C). This could be explained by the fact that THP1 null cells have already differentiated into macrophages, which respond to various stimuli differently than monocytes.[66,67] We should also take into account that these cells are of leukemic origin, whose responses tend to be weaker and may not cover the full spectrum of responses typical of primary cells.[39,68] We confirmed the co-inductive effect of MDP only for already primed THP1-null cells, which was assessed to be based on the synergy of NOD2 and NLRP3 activation (Figure S6C and D).

In contrast, the co-inducing effect on NLRP3 was not observed when monocytes were exposed to TiO_2 in the presence of LPS. One reason for this could be the decrease in metabolic activity, as measured by the WST-1 assay (Figure 3B). Additionally, TiO_2 enhanced the LPS-based release of IL-10 (Figure 3D), which has already been confirmed to attenuate a proinflammatory response in monocytes.[69] It should be noted that we stimulated monocytes for 24 h, which is, in the case of LPS, considered to be chronic exposure. Such prolonged stimulation has been described to dampen the NLRP3 expression in macrophages, precisely by inducing IL-10.[70] This regulatory mechanism is particularly important for the TLR4-LPS-mediated pathway as its rampant activity contributes to exacerbated production of proinflammatory cytokines, leading to a life-threatening condition called sepsis.[71] Adjusting the secretion of IL-10 then helps the macrophages to tame the ongoing inflammation.[72] As for the potentiating role of TiO_2, Bianchi et al found that binding of LPS to biocorona of TiO_2 P25 nanoparticles caused its enhanced activity.[37] Moreover, the uptake of such contaminated nanoparticles was found to be more efficient,[73] suggesting that TiO_2 serves as a Trojan horse for LPS. Therefore, the potentiating effect on IL-10 arises from the increased concentration of LPS in the cells.

To avoid the possible Trojan horse effect, we treated monocytes with LPS and MDP after TiO_2 removal. For both microbial stimuli, we found significantly increased IL-10 production when the cells were pretreated with TiO_2 (Figure 5), indicating that TiO_2 alone contributed to the regulatory response. The production of IL-1β in response to LPS was inhibited, even in the inflammatory model using the MDP-TiO_2 mixture (Figure 5B). The absence of elevated IL-1β levels in response to MDP treatment also clarified the necessity of the priming step before or concurrent with TiO_2-based

NLRP3 activation (Figure 5A). Furthermore, this result suggests that TiO_2-based stress signals in monocytes occur during initial processing and are rapidly compensated. As mentioned above, LPS alone is highly efficient proinflammatory inductor that also contributes to ROS generation and may cause cell death in a form of pyroptosis.[62] Like MDP, the initial reaction of monocytes is the activation of NLRP3.[60] However, when administered with TiO_2, which represents another stress signal, the compensatory response must be far more effective, in order to maintain homeostasis. This regulation may contribute to elevated IL-10 production. An eventual mechanism could be the augmented activation of cAMP response element-binding protein (CREB), a transcription factor involved in dampening the production of proinflammatory cytokines and inducing the expression of genes with anti-inflammatory and antioxidant effects.[74,75] Sanin et al postulated that the quick induction of IL-10 upon ligation of TLR4 and TLR2 depends on activation of CREB downstream via the phosphorylation of mitogen-activated protein kinases (MAPKs) p38 and ERK1/2.[76] The synergistic effect of TiO_2 and LPS on the on the phosphorylation of p38 has been previously documented in RAW264.7 macrophages.[36,37] The Inhibition of CREB in our study caused a small temporary leakage of LDH from TiO_2-treated monocytes, indicating a failure of compensatory mechanisms (Figure 6A). Moreover, LPS-mediated IL-10 production was also blocked (Figure 6B). CREB activation has been previously linked to scavenger receptors, particularly the SR-A family, which mediates one of the mechanisms of TiO_2 uptake.[77] Whether TiO_2 directly activates CREB downstream via ROS[78] or whether there is an indirect activation associated with TiO_2 uptake remains unclear. Nevertheless, CREB activity has been also associated with monocyte survival and differentiation to macrophages,[79] which we observed as well (Figure 7).

Based on previous findings, we can speculate whether these regulatory processes would affect monocytes in the long term, particularly during differentiation. Several studies have confirmed that IL-10 secreting monocytes preferentially differentiate into anti-inflammatory (regulatory) M2 subset of macrophages.[80] Sulahian et al found that IL-10 upregulates CD163, a scavenger receptor for hemoglobin-haptoglobin complex associated with the subset of anti-inflammatory M2c macrophages.[81,82] Although TiO_2 alone did not cause substantial IL-10 release (Figures 3D and S4B), it could still shift monocytes towards M2 subset. To evaluate this, we allowed the TiO_2-loaded monocytes to differentiate into macrophages. Flow cytometry confirmed that macrophages, which differentiated from TiO_2-treated monocytes, expressed CD64, CD163, CD206, and CD209 at a significantly higher rate than control cells, indicating the prevailing regulatory M2-like phenotype (Figure 7D).[83] The population was not homogenous, as a smaller subset with lower expression of CD14 but considerably higher expression of CD206, was present too. Further research is required to gain a better understanding of the inflammatory response of these modulated macrophages, as it seems that the accumulation of TiO_2 would result in altered inflammatory response affecting future infections. Additionally, possible alteration of innate immune memory should be considered as well. Such modulation has the potential to result in either an exacerbated or an insufficient reaction, which could ultimately lead to the development of chronic inflammation.

It is evident that TiO_2 uptake by monocytes might determine not only their physiological proinflammatory response, but also their differentiation into macrophages or dendritic cells after entering tissues. The in vivo study by Getts et al confirms that direct modulation of proinflammatory monocytes by specific particles may contribute to reducing symptoms of immunopathology-based diseases, as those monocytes no longer accumulate in inflammatory foci.[84] On the other hand, the uncontrolled modulation of monocytes into M2 macrophages may be associated with the rise of tumor associated macrophages (TAMs), thus fostering tumor environment.[85] It is clear that any potential modulatory effect of NPs, particularly those that are not acutely cytotoxic, on these cells must be carefully considered. In our study, we focused on NLRP3 as a main mechanism of NPs induced inflammatory potential, but the production of other cytokines and chemokines should be evaluated as well.

Conclusion

Our study confirmed that TiO_2 P25 had a non-negligible modulatory effect on primary monocytes in their inflammasome-based responses and their ability to differentiate. According to our results, intracellular processing of TiO_2 results in a pro-inflammatory "boost", which, however, does not have to be immediately apparent; that is, the absence of cytotoxicity and pro-inflammatory cytokines. Interestingly, this trigger has been shown to modulate the NLRP3-based response depending on the character of the bacterial costimulant, suggesting the participation of several molecular pathways based on the crosstalk between the transcriptional factors NF-κB and CREB. In addition, monocyte effort to compensate for this trigger may

ultimately lead to dampening inflammation and subsequent changes in differentiation towards M2 subsets of macrophages. Taken together, these results clearly indicate that primary monocytes represent an ideal model for testing immunomodulatory potential, and should not be neglected, particularly in the field of nanomedicine.

Acknowledgments

The authors thank Moeina Afshari for proofreading this manuscript.

Funding

This work was supported by the internal project of the University Hospital in Hradec Kralove, MH CZ-DRO UHHK, 00179906, and by institutional support from Charles University, Faculty of Medicine in Hradec Kralove: Cooperation Program, Research Area IMMU. The support of ERDF Project "NANOBIO" No. CZ.02.1.01/0.0/0.0/17_048/0007421 and Ministry of Education, Youth and Sports of Czech Republic project "CEREBIT" No. CZ.02.1.01/0.0/0.0/16_025/0007397 are also acknowledged.

Disclosure

The authors report no conflicts of interest in this work.

References

1. Jafari S, Mahyad B, Hashemzadeh H, Janfaza S, Gholikhani T, Tayebi L. Biomedical applications of TiO(2) nanostructures: recent advances. *Int J Nanomed*. 2020;15:3447–3470. doi:10.2147/IJN.S249441
2. Vaudagna MV, Aiassa V, Marcotti A, et al. Titanium Dioxide Nanoparticles in sunscreens and skin photo-damage. Development, synthesis and characterization of a novel biocompatible alternative based on their in vitro and in vivo study. *J Photochem Photobiol*. 2023;15:100173. doi:10.1016/j.jpap.2023.100173
3. Boutillier S, Fourmentin S, Laperche B. History of titanium dioxide regulation as a food additive: a review. *Environ Chem Lett*. 2022;20(2):1017–1033. doi:10.1007/s10311-021-01360-2
4. NIOSH. Current intelligence bulletin 63: occupational exposure to titanium dioxide. current intelligence bulletin 63. US Department of Health and Human Services, Centers for Disease Control and Prevention, National Institute for Occupational Safety and Health; 2011:2011–2160.
5. Fiordaliso F, Bigini P, Salmona M, Diomede L. Toxicological impact of titanium dioxide nanoparticles and food-grade titanium dioxide (E171) on human and environmental health. *Environ Sci*. 2022;9(4):1199–1211.
6. Ziental D, Czarczynska-Goslinska B, Mlynarczyk DT, et al. Titanium dioxide nanoparticles: prospects and applications in medicine. *Nanomaterials*. 2020;10(2):387. doi:10.3390/nano10020387
7. Pele LC, Thoree V, Bruggraber SF, et al. Pharmaceutical/food grade titanium dioxide particles are absorbed into the bloodstream of human volunteers. *Part Fibre Toxicol*. 2015;12:26. doi:10.1186/s12989-015-0101-9
8. Pujalté I, Dieme D, Haddad S, Serventi AM, Bouchard M. Toxicokinetics of titanium dioxide (TiO2) nanoparticles after inhalation in rats. *Toxicol Lett*. 2017;265:77–85. doi:10.1016/j.toxlet.2016.11.014
9. Akagi J-I, Mizuta Y, Akane H, Toyoda T, Ogawa K. Oral toxicological study of titanium dioxide nanoparticles with a crystallite diameter of 6 nm in rats. *Part Fibre Toxicol*. 2023;20(1):23. doi:10.1186/s12989-023-00533-x
10. Bachler G, von Goetz N, Hungerbuhler K. Using physiologically based pharmacokinetic (PBPK) modeling for dietary risk assessment of titanium dioxide (TiO2) nanoparticles. *Nanotoxicology*. 2015;9(3):373–380. doi:10.3109/17435390.2014.940404
11. Geraets L, Oomen AG, Krystek P, et al. Tissue distribution and elimination after oral and intravenous administration of different titanium dioxide nanoparticles in rats. *Part Fibre Toxicol*. 2014;11(1):30. doi:10.1186/1743-8977-11-30
12. Shinohara N, Danno N, Ichinose T, et al. Tissue distribution and clearance of intravenously administered titanium dioxide (TiO2) nanoparticles. *Nanotoxicology*. 2014;8(2):132–141. doi:10.3109/17435390.2012.763001
13. Elgrabli D, Beaudouin R, Jbilou N, et al. Biodistribution and clearance of TiO2 nanoparticles in rats after intravenous injection. *PLoS One*. 2015;10(4):e0124490. doi:10.1371/journal.pone.0124490
14. Mbanga O, Cukrowska E, Gulumian M. Dissolution of titanium dioxide nanoparticles in synthetic biological and environmental media to predict their biodurability and persistence. *Toxicol In Vitro*. 2022;84:105457. doi:10.1016/j.tiv.2022.105457
15. Farrera C, Fadeel B. It takes two to tango: understanding the interactions between engineered nanomaterials and the immune system. *Eur J Pharm Biopharm*. 2015;95(Pt A):3–12. doi:10.1016/j.ejpb.2015.03.007
16. Gustafson HH, Holt-Casper D, Grainger DW, Ghandehari H. Nanoparticle Uptake: the Phagocyte Problem. *Nano Today*. 2015;10(4):487–510. doi:10.1016/j.nantod.2015.06.006
17. Hewitt RE, Vis B, Pele LC, Faria N, Powell JJ. Imaging flow cytometry assays for quantifying pigment grade titanium dioxide particle internalization and interactions with immune cells in whole blood. *Cytometry A*. 2017;91(10):1009–1020. doi:10.1002/cyto.a.23245
18. Ziegler-Heitbrock L, Ancuta P, Crowe S, et al. Nomenclature of monocytes and dendritic cells in blood. *Blood*. 2010;116(16):e74–80. doi:10.1182/blood-2010-02-258558
19. Luebke R. Immunotoxicant screening and prioritization in the twenty-first century. *Toxicol Pathol*. 2012;40(2):294–299. doi:10.1177/0192623311427572
20. Li Z, Guo J, Bi L. Role of the NLRP3 inflammasome in autoimmune diseases. *Biomed Pharmacother*. 2020;130:110542. doi:10.1016/j.biopha.2020.110542

21. Swartzwelter BJ, Barbero F, Verde A, et al. Gold nanoparticles modulate BCG-induced innate immune memory in human monocytes by shifting the memory response towards tolerance. *Cells*. 2020;9(2):284. doi:10.3390/cells9020284
22. Beyeler S, Steiner S, Wotzkow C, et al. Multi-walled carbon nanotubes activate and shift polarization of pulmonary macrophages and dendritic cells in an in vivo model of chronic obstructive lung disease. *Nanotoxicology*. 2020;14(1):77–96. doi:10.1080/17435390.2019.1663954
23. Svadlakova T, Kolackova M, Vankova R, et al. Carbon-based nanomaterials increase reactivity of primary monocytes towards various bacteria and modulate their differentiation into macrophages. *Nanomaterials*. 2021;11(10):2510. doi:10.3390/nano11102510
24. Jetten N, Verbruggen S, Gijbels MJ, Post MJ, De Winther MPJ, Donners MMPC. Anti-inflammatory M2, but not pro-inflammatory M1 macrophages promote angiogenesis in vivo. *Angiogenesis*. 2014;17(1):109–118. doi:10.1007/s10456-013-9381-6
25. Lendeckel U, Venz S, Wolke C. Macrophages: shapes and functions. *ChemTexts*. 2022;8(2):12. doi:10.1007/s40828-022-00163-4
26. Netea MG, Domínguez-Andrés J, Barreiro LB, et al. Defining trained immunity and its role in health and disease. *Nat Rev Immunol*. 2020;20 (6):375–388. doi:10.1038/s41577-020-0285-6
27. Murray Peter J, Allen Judith E, Biswas Subhra K, et al. Macrophage activation and polarization: nomenclature and experimental guidelines. *Immunity*. 2014;41(1):14–20. doi:10.1016/j.immuni.2014.06.008
28. Lebre F, Boland JB, Gouveia P, et al. Pristine graphene induces innate immune training. *Nanoscale*. 2020;12(20):11192–11200. doi:10.1039/C9NR09661B
29. Alsaleh NB, Minarchick VC, Mendoza RP, Sharma B, Podila R, Brown JM. Silver nanoparticle immunomodulatory potential in absence of direct cytotoxicity in RAW 264.7 macrophages and MPRO 2.1 neutrophils. *J Immunotoxicol*. 2019;16(1):63–73. doi:10.1080/1547691X.2019.1588928
30. Bacova J, Knotek P, Kopecka K, et al. Evaluating the use of TiO(2) nanoparticles for toxicity testing in pulmonary A549 cells. *Int J Nanomed*. 2022;17:4211–4225. doi:10.2147/IJN.S374955
31. Schoenenberger AD, Schipanski A, Malheiro V, et al. Macrophage polarization by titanium dioxide (TiO(2)) particles: size matters. *ACS Biomater Sci Eng*. 2016;2(6):908–919. doi:10.1021/acsbiomaterials.6b00006
32. Kolling J, Tigges J, Hellack B, Albrecht C, Schins RPF. Evaluation of the NLRP3 inflammasome activating effects of a large panel of TiO(2) nanomaterials in macrophages. *Nanomaterials*. 2020;10(9):1876. doi:10.3390/nano10091876
33. Lehotska Mikusova M, Busova M, Tulinska J, et al. Titanium dioxide nanoparticles modulate systemic immune response and increase levels of reduced glutathione in mice after seven-week inhalation. *Nanomaterials*. 2023;13(4):767. doi:10.3390/nano13040767
34. Morishige T, Yoshioka Y, Tanabe A, et al. Titanium dioxide induces different levels of IL-1beta production dependent on its particle characteristics through caspase-1 activation mediated by reactive oxygen species and cathepsin B. *Biochem Biophys Res Commun*. 2010;392(2):160–165. doi:10.1016/j.bbrc.2009.12.178
35. Huang C, Sun M, Yang Y, et al. Titanium dioxide nanoparticles prime a specific activation state of macrophages. *Nanotoxicology*. 2017;11 (6):737–750. doi:10.1080/17435390.2017.1349202
36. Bianchi MG, Allegri M, Costa AL, et al. Titanium dioxide nanoparticles enhance macrophage activation by LPS through a TLR4-dependent intracellular pathway. *Toxicol Res*. 2015;4(2):385–398. doi:10.1039/C4TX00193A
37. Bianchi MG, Allegri M, Chiu M, et al. Lipopolysaccharide adsorbed to the bio-corona of TiO(2) nanoparticles powerfully activates selected pro-inflammatory transduction pathways. *Front Immunol*. 2017;8:866. doi:10.3389/fimmu.2017.00866
38. Tsugita M, Morimoto N, Nakayama M. SiO(2) and TiO(2) nanoparticles synergistically trigger macrophage inflammatory responses. *Part Fibre Toxicol*. 2017;14(1):11. doi:10.1186/s12989-017-0192-6
39. Tedesco S, De Majo F, Kim J, et al. Convenience versus biological significance: are PMA-differentiated THP-1 cells a reliable substitute for blood-derived macrophages when studying in vitro polarization? *Front Pharmacol*. 2018;9:71. doi:10.3389/fphar.2018.00071
40. Scherbart AM, Langer J, Bushmelev A, et al. Contrasting macrophage activation by fine and ultrafine titanium dioxide particles is associated with different uptake mechanisms. *Part Fibre Toxicol*. 2011;8:31. doi:10.1186/1743-8977-8-31
41. Della Camera G, Liu T, Yang W, et al. Induction of innate memory in human monocytes exposed to mixtures of bacterial agents and nanoparticles. *Int J Mol Sci*. 2022;23(23):14655. doi:10.3390/ijms232314655
42. Lessard AJ, LeBel M, Egarnes B, et al. Triggering of NOD2 receptor converts inflammatory Ly6C(high) into Ly6C(low) monocytes with patrolling properties. *Cell Rep*. 2017;20(8):1830–1843. doi:10.1016/j.celrep.2017.08.009
43. Hussain S, Vanoirbeek JA, Hoet PH. Interactions of nanomaterials with the immune system. *Wiley Interdiscip Rev Nanomed Nanobiotechnol*. 2012;4(2):169–183. doi:10.1002/wnan.166
44. Dobrovolskaia MA, McNeil SE. Immunological properties of engineered nanomaterials. *Nat Nanotechnol*. 2007;2(8):469–478. doi:10.1038/nnano.2007.223
45. Svadlakova T, Holmannova D, Kolackova M, Malkova A, Krejsek J, Fiala Z. Immunotoxicity of carbon-based nanomaterials, starring phagocytes. *Int J Mol Sci*. 2022;23(16):8889. doi:10.3390/ijms23168889
46. Ginhoux F, Jung S. Monocytes and macrophages: developmental pathways and tissue homeostasis. *Nat Rev Immunol*. 2014;14(6):392–404. doi:10.1038/nri3671
47. Ruppert J, Schütt C, Ostermeier D, Peters JH. Down-regulation and release of CD14 on human monocytes by IL-4 depends on the presence of serum or GM-CSF. *Adv Exp Med Biol*. 1993;329:281–286.
48. Hunter M, Wang Y, Eubank T, Baran C, Nana-Sinkam P, Marsh C. Survival of monocytes and macrophages and their role in health and disease. *Front Biosci*. 2009;14(11):4079–4102. doi:10.2741/3514
49. Bhattacharya A, Ghosh P, Singh A, et al. Delineating the complex mechanistic interplay between NF-κβ driven mTOR depedent autophagy and monocyte to macrophage differentiation: a functional perspective. *Cell Signal*. 2021;88:110150. doi:10.1016/j.cellsig.2021.110150
50. Svadlakova T, Hubatka F, Turanek Knotigova P, et al. Proinflammatory effect of carbon-based nanomaterials: in vitro study on stimulation of inflammasome NLRP3 via destabilisation of lysosomes. *Nanomaterials*. 2020;10(3):418. doi:10.3390/nano10030418
51. Grosse S, Stenvik J, Nilsen AM. Iron oxide nanoparticles modulate lipopolysaccharide-induced inflammatory responses in primary human monocytes. *Int J Nanomed*. 2016;11:4625–4642. doi:10.2147/IJN.S113425
52. Suri SS, Fenniri H, Singh B. Nanotechnology-based drug delivery systems. *J Occup Med Toxicol*. 2007;2:16. doi:10.1186/1745-6673-2-16
53. Sharma B, McLeland CB, Potter TM, Stern ST, Adiseshaiah PP. Assessing NLRP3 Inflammasome Activation by Nanoparticles. In: McNeil SE, editor. *Characterization of Nanoparticles Intended for Drug Delivery*. New York: Springer New York; 2018:135–147.

54. Knötigová PT, Mašek J, Hubatka F, et al. Application of advanced microscopic methods to study the interaction of carboxylated fluorescent nanodiamonds with membrane structures in THP-1 cells: activation of inflammasome NLRP3 as the result of lysosome destabilization. *Mol Pharm*. 2019;16:3441–3451. doi:10.1021/acs.molpharmaceut.9b00225
55. Sun B, Wang X, Ji Z, Li R, Xia T. NLRP3 inflammasome activation induced by engineered nanomaterials. *Small*. 2013;9(9–10):1595–1607. doi:10.1002/smll.201201962
56. Abbasi-Oshaghi E, Mirzaei F, Pourjafar M. NLRP3 inflammasome, oxidative stress, and apoptosis induced in the intestine and liver of rats treated with titanium dioxide nanoparticles: in vivo and in vitro study. *Int J Nanomed*. 2019;14:1919–1936. doi:10.2147/IJN.S192382
57. Baron L, Gombault A, Fanny M, et al. The NLRP3 inflammasome is activated by nanoparticles through ATP, ADP and adenosine. *Cell Death Dis*. 2015;6(2):e1629. doi:10.1038/cddis.2014.576
58. He Y, Hara H, Nunez G. Mechanism and regulation of NLRP3 inflammasome activation. *Trends Biochem Sci*. 2016;41(12):1012–1021. doi:10.1016/j.tibs.2016.09.002
59. Unterberger S, Mullen L, Flint MS, Sacre S. Multiple TLRs elicit alternative NLRP3 inflammasome activation in primary human monocytes independent of RIPK1 kinase activity. *Front Immunol*. 2023;14:1092799. doi:10.3389/fimmu.2023.1092799
60. Gritsenko A, Yu S, Martin-Sanchez F, et al. Priming is dispensable for NLRP3 inflammasome activation in human monocytes in vitro. *Front Immunol*. 2020:11. doi:10.3389/fimmu.2020.00011
61. Gojznikar J, Zdravković B, Vidak M, Leskošek B, Ferk P. TiO(2) nanoparticles and their effects on eukaryotic cells: a double-edged sword. *Int J Mol Sci*. 2022;23(20):12353. doi:10.3390/ijms232012353
62. Groslambert M, Py BF. Spotlight on the NLRP3 inflammasome pathway. *J Inflamm Res*. 2018;11:359–374. doi:10.2147/JIR.S141220
63. Akbal A, Dernst A, Lovotti M, Mangan MSJ, McManus RM, Latz E. How location and cellular signaling combine to activate the NLRP3 inflammasome. *Cell Mol Immunol*. 2022;19(11):1201–1214. doi:10.1038/s41423-022-00922-w
64. Negroni A, Pierdomenico M, Cucchiara S, Stronati L. NOD2 and inflammation: current insights. *J Inflamm Res*. 2018;11:49–60. doi:10.2147/JIR.S137606
65. Martinon F, Agostini L, Meylan E, Tschopp J. Identification of bacterial muramyl dipeptide as activator of the NALP3/cryopyrin inflammasome. *Curr Biol*. 2004;14(21):1929–1934. doi:10.1016/j.cub.2004.10.027
66. Guo Y, Zhao G, Tanaka S, Yamaguchi T. Differential responses between monocytes and monocyte-derived macrophages for lipopolysaccharide stimulation of calves. *Cell Mol Immunol*. 2009;6(3):223–229. doi:10.1038/cmi.2009.30
67. Austermann J, Roth J, Barczyk-Kahlert K. The good and the bad: monocytes' and macrophages' diverse functions in inflammation. *Cells*. 2022;11 (12):1979. doi:10.3390/cells11121979
68. Schildberger A, Rossmanith E, Eichhorn T, Strassl K, Weber V. Monocytes, peripheral blood mononuclear cells, and THP-1 cells exhibit different cytokine expression patterns following stimulation with lipopolysaccharide. *Mediators Inflamm*. 2013;2013:697972. doi:10.1155/2013/697972
69. Byrne A, Reen DJ. Lipopolysaccharide induces rapid production of IL-10 by monocytes in the presence of apoptotic neutrophils. *J Immunol*. 2002;168(4):1968–1977. doi:10.4049/jimmunol.168.4.1968
70. Gurung P, Li B, Subbarao Malireddi RK, Lamkanfi M, Geiger TL, Kanneganti TD. Chronic TLR stimulation controls NLRP3 inflammasome activation through IL-10 mediated regulation of NLRP3 expression and caspase-8 activation. *Sci Rep*. 2015;5:14488. doi:10.1038/srep14488
71. Mbongue JC, Vanterpool E, Firek A, Langridge WHR. Lipopolysaccharide-induced immunological tolerance in monocyte-derived dendritic cells. *Immuno*. 2022;2(3):482–500. doi:10.3390/immuno2030030
72. Kessler B, Rinchai D, Kewcharoenwong C, et al. Interleukin 10 inhibits pro-inflammatory cytokine responses and killing of Burkholderia pseudomallei. *Sci Rep*. 2017;7(1):42791. doi:10.1038/srep42791
73. Lahiani MH, Gokulan K, Williams K, Khodakovskaya MV, Khare S. Graphene and carbon nanotubes activate different cell surface receptors on macrophages before and after deactivation of endotoxins. *J Appl Toxicol*. 2017;37(11):1305–1316. doi:10.1002/jat.3477
74. Larabee JL, Hauck G, Ballard JD. Unique, intersecting, and overlapping roles of C/EBP β and CREB in cells of the innate immune system. *Sci Rep*. 2018;8(1):16931. doi:10.1038/s41598-018-35184-y
75. Lee B, Cao R, Choi YS, et al. The CREB/CRE transcriptional pathway: protection against oxidative stress-mediated neuronal cell death. *J Neurochem*. 2009;108(5):1251–1265. doi:10.1111/j.1471-4159.2008.05864.x
76. Sanin DE, Prendergast CT, Mountford AP. IL-10 production in macrophages is regulated by a TLR-driven CREB-mediated mechanism that is linked to genes involved in cell metabolism. *J Immunol*. 2015;195(3):1218–1232. doi:10.4049/jimmunol.1500146
77. Arredouani M, Yang Z, Ning Y, et al. The scavenger receptor MARCO is required for lung defense against pneumococcal pneumonia and inhaled particles. *J Exp Med*. 2004;200(2):267–272. doi:10.1084/jem.20040731
78. Wen AY, Sakamoto KM, Miller LS. The role of the transcription factor CREB in immune function. *J Immunol*. 2010;185(11):6413–6419. doi:10.4049/jimmunol.1001829
79. Cheng JC, Kinjo K, Judelson DR, et al. CREB is a critical regulator of normal hematopoiesis and leukemogenesis. *Blood*. 2008;111(3):1182–1192. doi:10.1182/blood-2007-04-083600
80. Prasse A, Germann M, Pechkovsky DV, et al. IL-10-producing monocytes differentiate to alternatively activated macrophages and are increased in atopic patients. *J Allergy Clin Immunol*. 2007;119(2):464–471. doi:10.1016/j.jaci.2006.09.030
81. Sulahian TH, Högger P, Wahner AE, et al. Human monocytes express CD163, which is upregulated by IL-10 and identical to p155. *Cytokine*. 2000;12(9):1312–1321. doi:10.1006/cyto.2000.0720
82. Philippidis P, Mason JC, Evans BJ, et al. Hemoglobin scavenger receptor CD163 mediates interleukin-10 release and heme oxygenase-1 synthesis: antiinflammatory monocyte-macrophage responses in vitro, in resolving skin blisters in vivo, and after cardiopulmonary bypass surgery. *Circ Res*. 2004;94(1):119–126. doi:10.1161/01.RES.0000109414.78907.F9
83. Strizova Z, Benesova I, Bartolini R, et al. M1/M2 macrophages and their overlaps - myth or reality? *Clin Sci*. 2023;137(15):1067–1093. doi:10.1042/CS20220531
84. Getts DR, Terry RL, Getts MT, et al. Therapeutic inflammatory monocyte modulation using immune-modifying microparticles. *Sci Transl Med*. 2014;6(219):219ra217. doi:10.1126/scitranslmed.3007563
85. Wang S, Wang J, Chen Z, et al. Targeting M2-like tumor-associated macrophages is a potential therapeutic approach to overcome antitumor drug resistance. *NPJ Precis Oncol*. 2024;8(1):31. doi:10.1038/s41698-024-00522-z